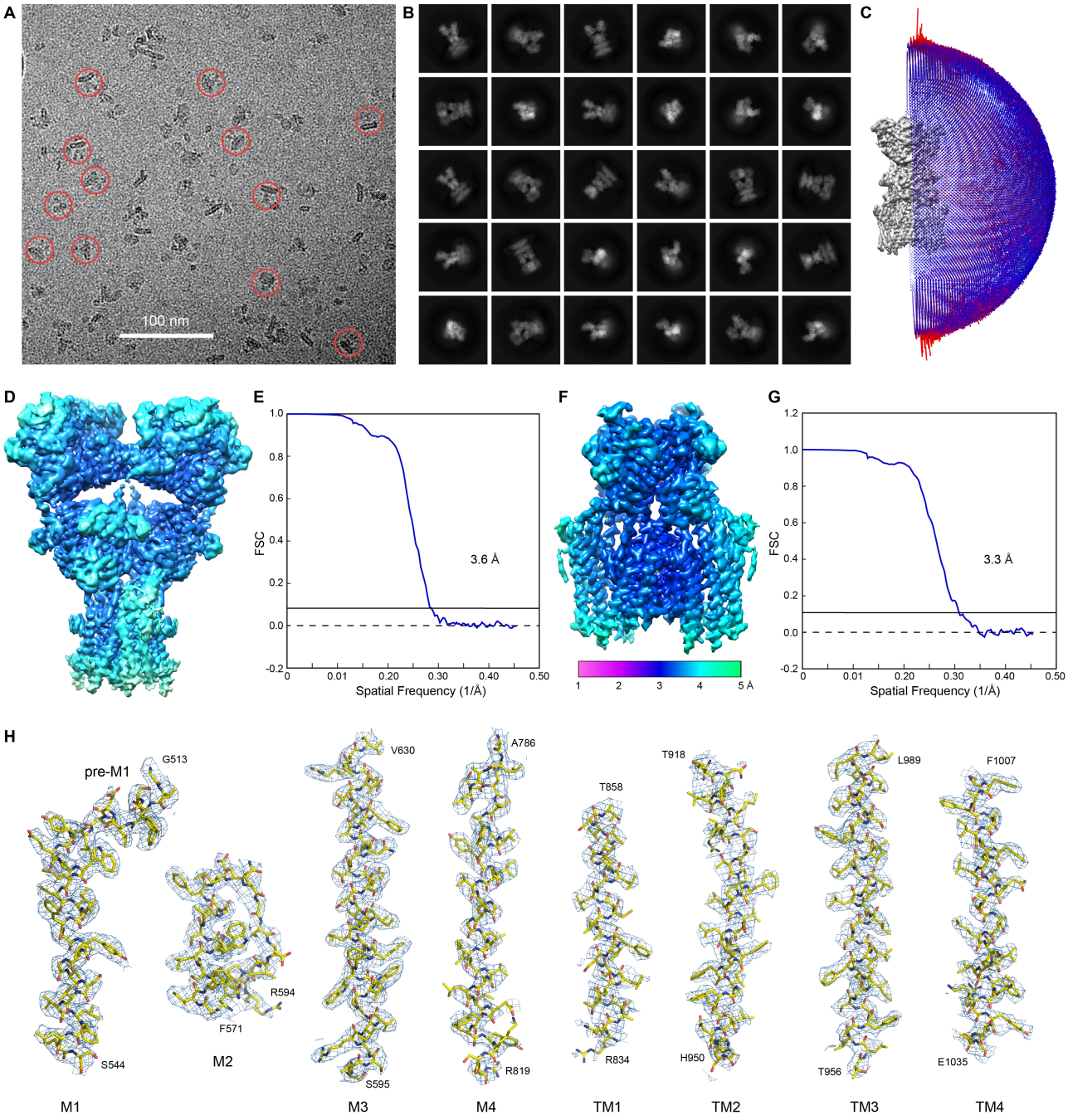

Figure S1. Overview of single-particle cryo-EM for GluA2-γ5 in complex with competitive antagonist ZK200775, Related to Figure 1

A. Representative micrograph with example particles circled in red. B. Reference-free 2D class averages illustrating different particle orientations. C. Distribution of particle Euler angle orientations contributing to the final reconstruction, with larger red cylinders representing orientations comprising more particles. D-G. Local resolution presented as coloring of the cryo-EM map (D and F) and FSC curves (E and G) for the full-length (D and E) and LBD-TMD-focused (F and G) reconstructions of GluA2-γ5$_{ZK}$. H. Fragments of the 3.3-Å resolution LBD-TMD-focused GluA2-γ5$_{ZK}$ reconstruction map for GluA2 (M1-M4) and γ5 (TM1-TM4) membrane segments.

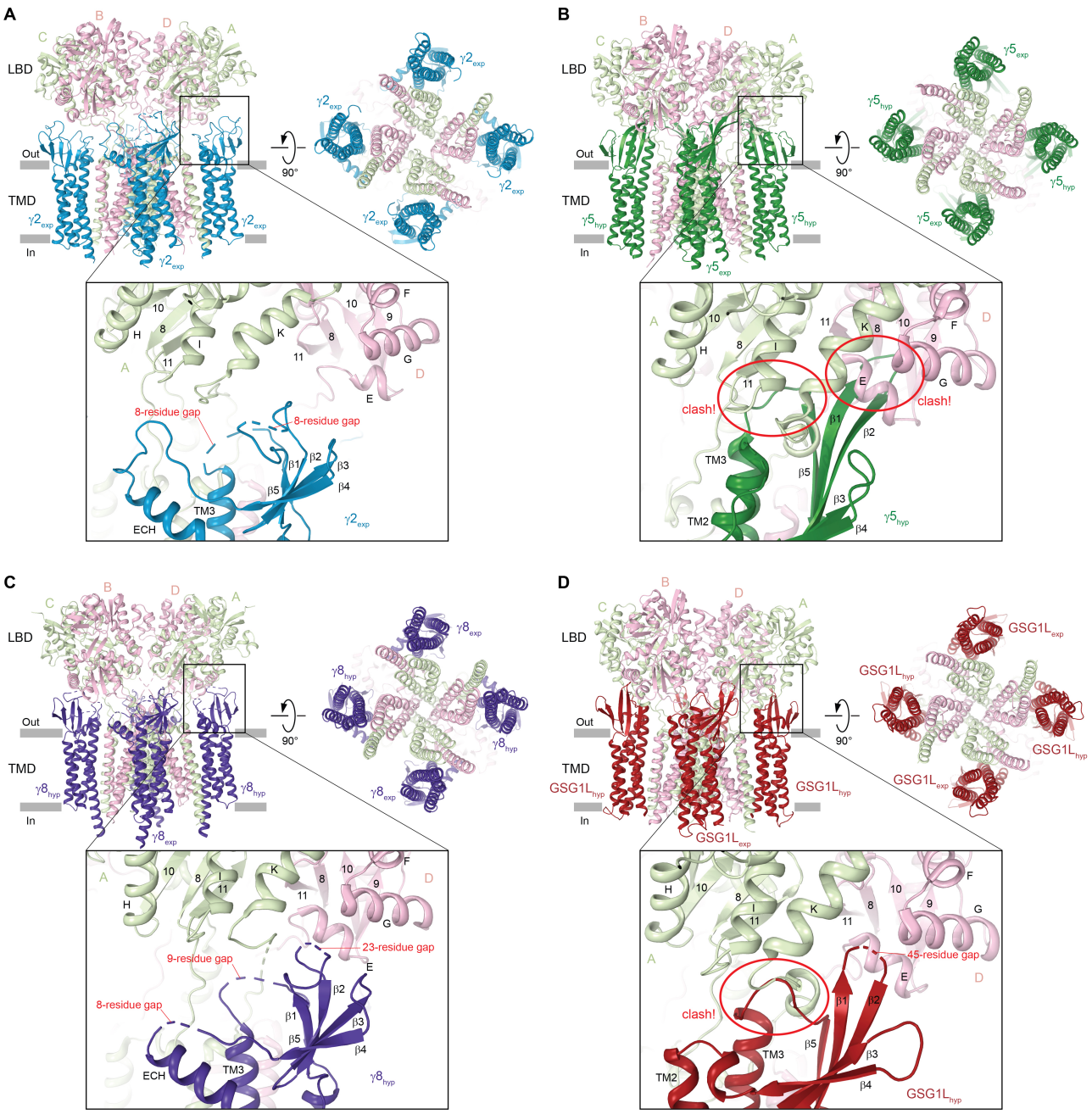

Figure S2. Probing stoichiometry of AMPA receptor-auxiliary subunit complexes using steric clash analysis, Related to Figure 2

A-D. LBD-TMD portions of AMPA receptor in complex with auxiliary subunits γ2 (A; PDB 5WEO), γ5 (B; GluA2-$\gamma5_{Quis}$), γ8 (C; PDB 7OCE) and GSG1L (D; GluA2-$GSG1L_{Quis}$) viewed parallel to the membrane (left) or intracellularly (right), with the contact regions between the head domains of auxiliary subunits and LBDs shown as insets. AMPA receptor subunits are colored light green and pink. The names of experimentally observed (exp) and hypothetical (hyp) auxiliary subunits are labeled with the corresponding subscripts. The hypothetical auxiliary subunits are obtained by rotating the experimental auxiliary subunits by 90° around the axis of ion channel 4-fold rotational symmetry. Obvious clashes are highlighted with red ovals. The numbers of residues that are missing in the loops of the auxiliary subunit structures are indicated.

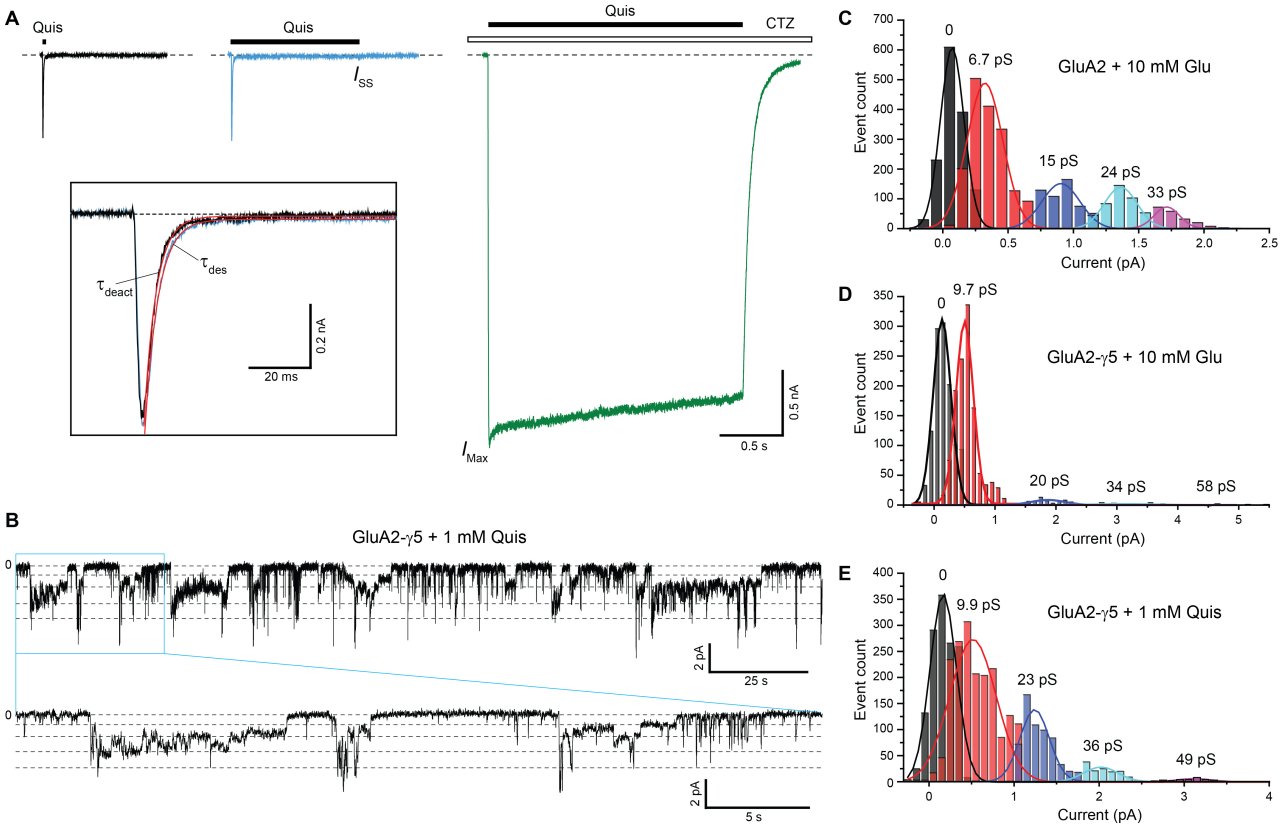

F

Construct / Ligand / Parameter	GluA2		$GluA2_{Mut}$	GluA2-γ5		$GluA2_{Mut}$-γ5	GluA2-GSG1L	
	Glu	Quis	Glu	Glu	Quis	Glu	Glu	Quis
I_{SS}/I_{Max}	0.042 ± 0.009 (n = 22)	0.031 ± 0.007 (n = 6)	0.042 ± 0.011 (n = 7)	0.0091 ± 0.0029 (n = 6)	0.0078 ± 0.0030 (n = 6)	0.029 ± 0.009 (n = 8)	0.032 ± 0.008 (n = 13)	0.023 ± 0.012 (n = 6)
τ_{Deact} (ms)	1.76 ± 0.24 (n = 9)	2.77 ± 0.19 (n = 8)	2.78 ± 0.20 (n = 4)	2.14 ± 0.15 (n = 8)	4.15 ± 0.25 (n = 6)	2.17 ± 0.08 (n = 7)	3.94 ± 0.43 (n = 11)	3.39 ± 0.32 (n = 11)
τ_{Des} (ms)	7.7 ± 0.4 (n = 31)	6.3 ± 0.4 (n = 9)	9.9 ± 0.8 (n = 6)	9.3 ± 0.8 (n = 7)	5.09 ± 0.33 (n = 11)	9.6 ± 0.4 (n = 8)	8.95 ± 0.85 (n = 17)	5.14 ± 0.36 (n = 14)
τ_{RecDes} (ms)	15.3 ± 1.1 (n = 14)	121 ± 7 (n = 5)	15.9 ± 0.7 (n = 5)	29.8 ± 1.9 (n = 6)	130 ± 4 (n = 10)	49.7 ± 3.0 (n = 6)	164 ± 11 (n = 7)	836 ± 31 (n = 8)

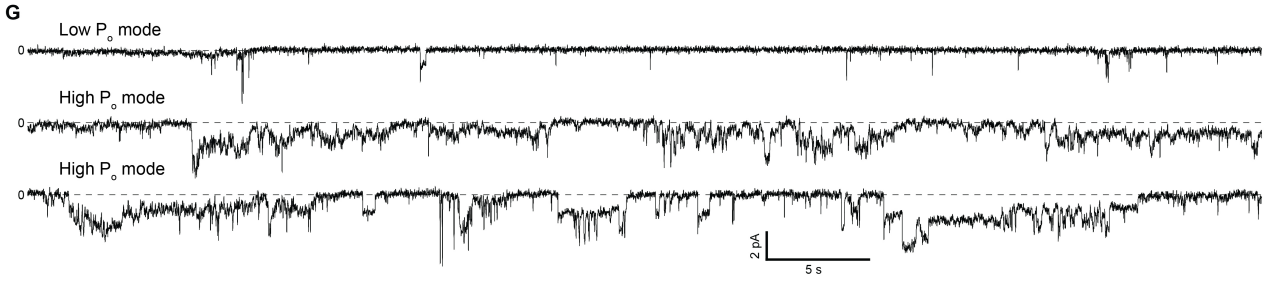

Figure S3. Activation of GluA2-γ5 by quisqualate and functional characterization of different constructs, Related to Figure 1

A. Representative whole-cell currents recorded at –60 mV membrane potential from HEK 293 cell expressing GluA2-γ5 in response to 2-ms (black) or 1-s (blue) applications of 1 mM Quis alone or 2-s application of Quis in the continuous presence of 30 μM CTZ (green). The inset shows normalized currents in response to 2-ms and 1-s applications of Quis alone fitted using single exponentials (red curves) with τ_{Deact} = 3.99 ± 0.25 ms and τ_{Des} = 4.40 ± 0.17 ms (mean ± SEM). B. Representative single-channel current recorded at –60 mV membrane potential in the continuous presence of 1 mM Quis and 100 μM CTZ from GluA2-γ5 reconstituted into the lipid bilayer (upper trace), with an expanded view of the region indicated by the blue box (lower trace). Horizontal dashed lines indicate different conductance levels. C-E. Example amplitude histograms of single channel events from individual experiments with GuA2 (C) or GluA2-γ5 (D-E) incorporated into planar lipid bilayers and activated by 10 mM Glu (C-D) or 1 mM Quis (E) in the continuous presence of 100 μM CTZ. Data was fitted with differently colored Gaussians, with the average conductance indicated above the corresponding components. F. Table of parameters. Shown are the non-desensitized fraction (I_{SS}/I_{Max}) and the time constants of deactivation (τ_{Deact}), desensitization (τ_{Des}) and recovery from desensitization (τ_{RecDes}). The data for GluA2 and GluA2-GSG1L have been published previously (Twomey et al., 2017b; Yelshanskaya et al., 2017). The values presented are mean ± SEM. G. Examples of low and high open probability modes that represent fragments of the same single-channel recording at –60 mV membrane potential from GluA2-γ5 reconstituted into the lipid bilayer in the presence of 1 mM Quis and 100 μM CTZ.

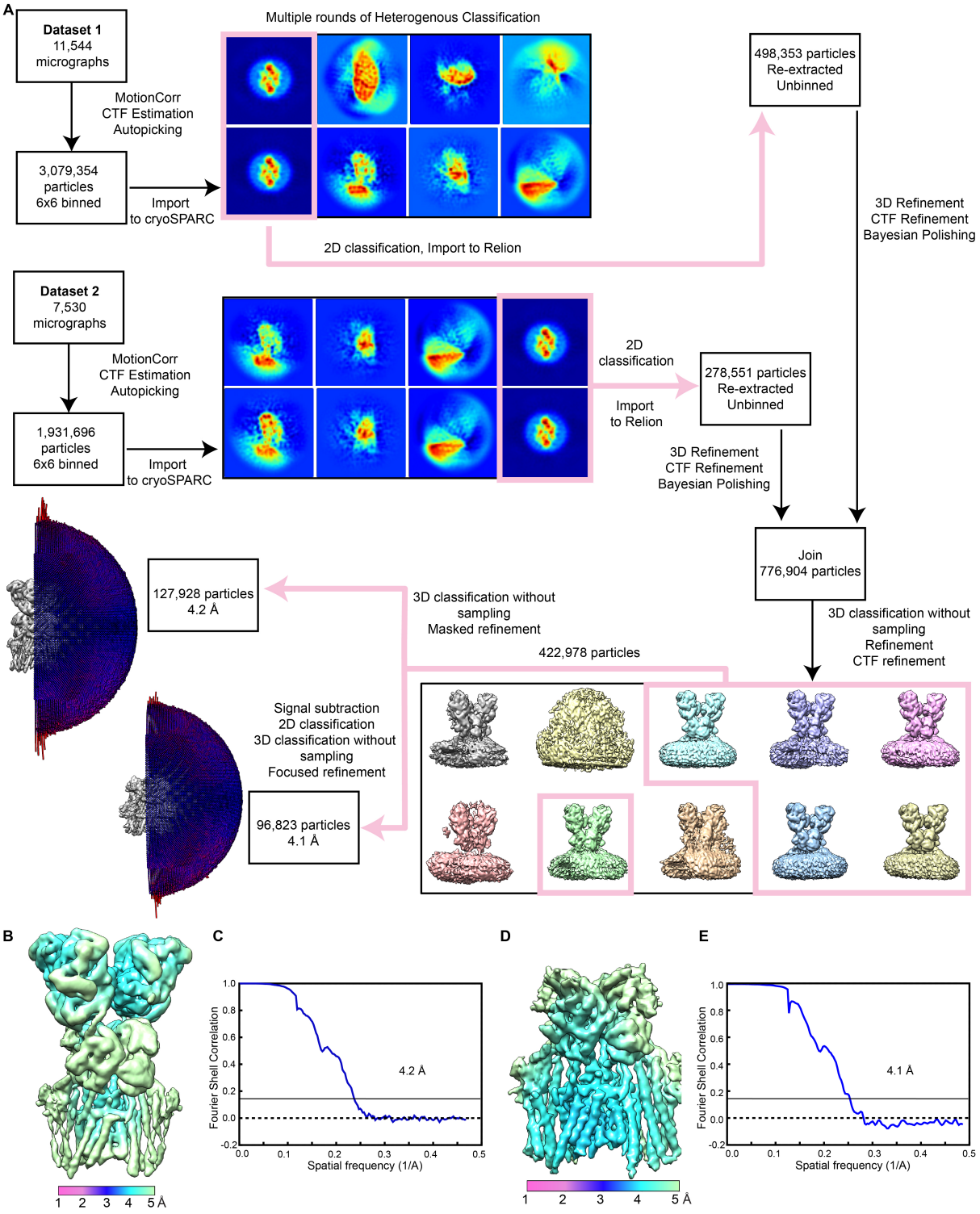

Figure S4. Overview of single-particle cryo-EM for GluA2-γ5 in complex with agonist quisqualate, Related to Figure 4

A. 3D reconstruction workflow involving Relion 3.1 and cryoSPARC. Included are distributions of particle Euler angle orientations contributing to the full-length and LBD-TMD-focused reconstructions of GluA2-γ5$_{Quis}$, with larger red cylinders representing orientations comprising more particles. B-E. Local resolution presented as coloring of the cryo-EM map (B and D) and FSC curves (C and E) for the full-length (B and C) and LBD-TMD-focused (D and E) reconstructions of GluA2-γ5$_{Quis}$.

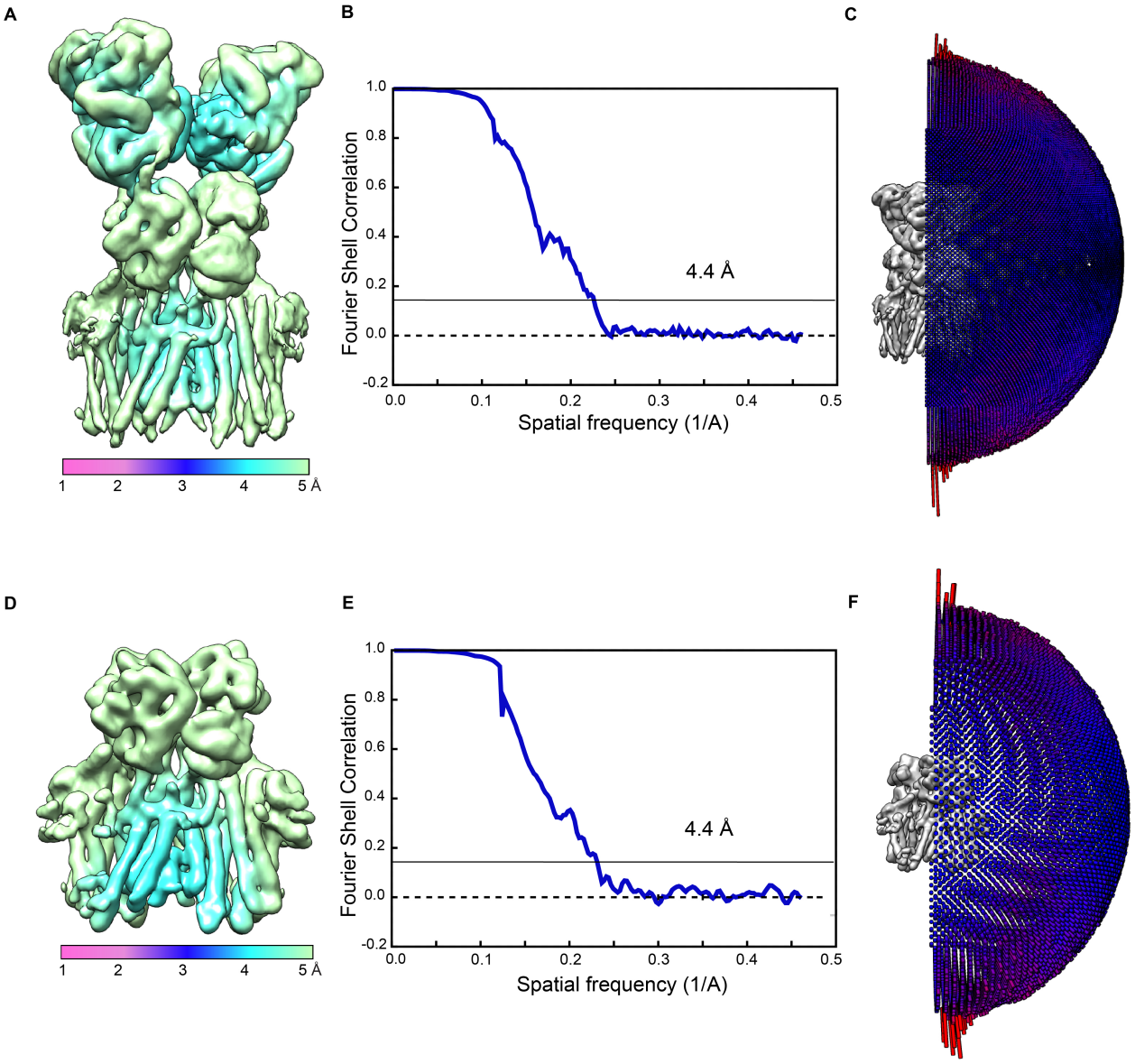

Figure S5. Overview of single-particle cryo-EM for GluA2-γ5 in complex with agonist glutamate, Related to Figure 4

A-F. Local resolution presented as coloring of the cryo-EM map (A and D), FSC curves (B and E), and distribution of particle Euler angle orientations contributing to the final reconstruction (C and F) for the full-length (A-C) and LBD-TMD-focused (D-F) reconstructions of GluA2-γ5$_{Glu}$.

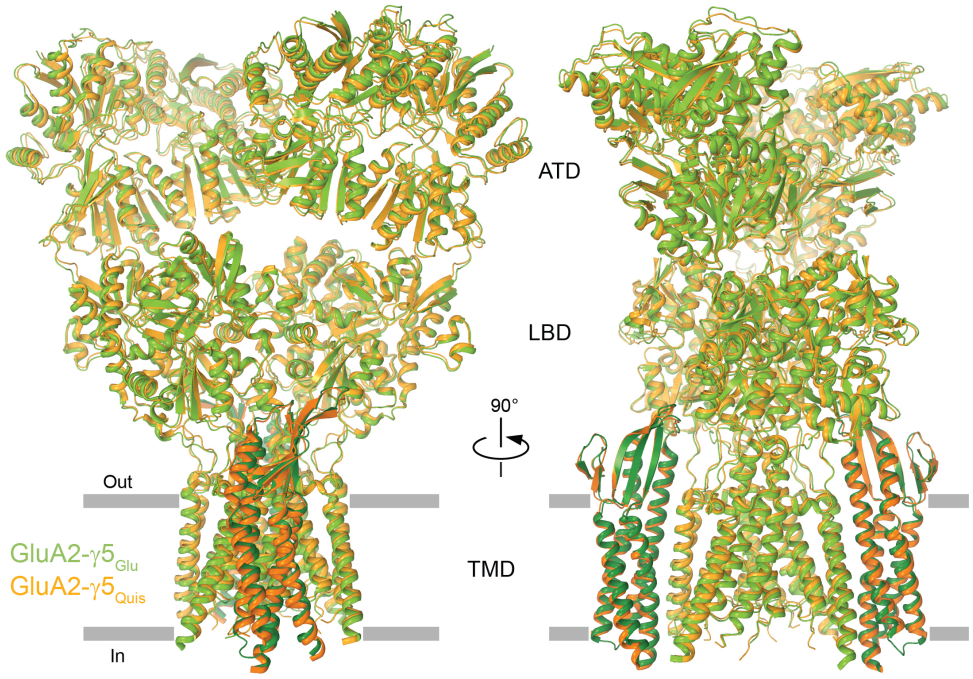

Figure S6. Comparison of GluA2-γ5$_{Glu}$ and GluA2-γ5$_{Quis}$ structures, Related to Figure 4

Superposition of GluA2-γ5$_{Glu}$ and GluA2-γ5$_{Quis}$ viewed parallel to the membrane, with GluA2 subunits shown in light green and orange, and γ5 in dark green and orange colors, respectively.

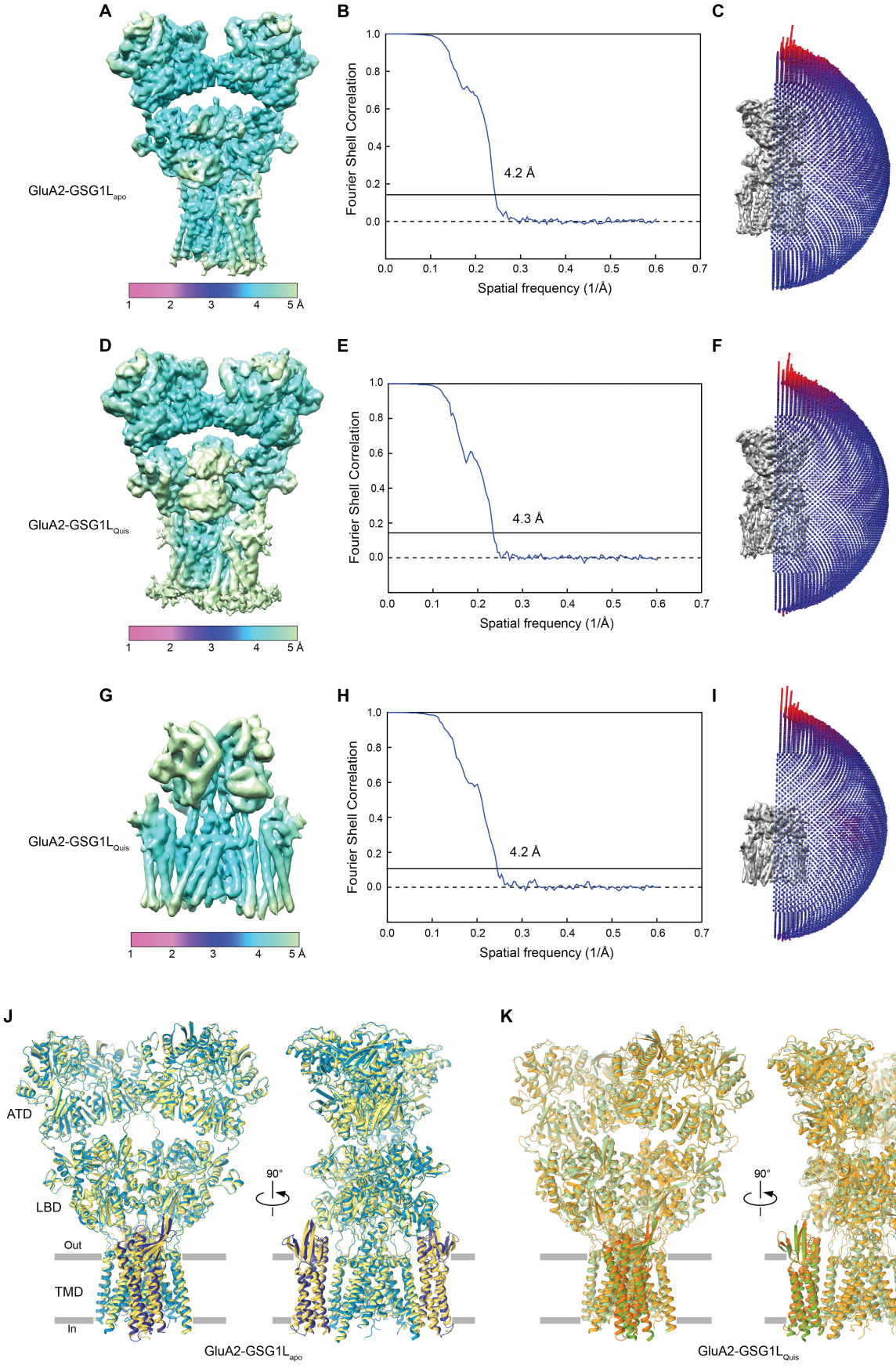
A
B
C
GluA2-GSG1L$_{apo}$
1 2 3 4 5 Å
Fourier Shell Correlation
4.2 Å
Spatial frequency (1/Å)
D
E
F
GluA2-GSG1L$_{Quis}$
4.3 Å
G
H
I
J
K
ATD
LBD
Out
TMD
In
90°
GluA2-GSG1L$_{apo}$
GluA2-GSG1L$_{Quis}$

Figure S7. Overview of cryo-EM and comparison of GluA2-GSG1L structures, Related to Figure 6

A-I. Local resolution presented as coloring of the cryo-EM map (A, D, and G), FSC curves (B, E, and H), and distribution of particle Euler angle orientations contributing to the final reconstruction (C, F, and I) for the full-length reconstruction of GluA2-GSG1L$_{apo}$ (A-C), and full-length (D-F) and LBD-TMD-focused (G-I) reconstructions of GluA2-GSG1L$_{Quis}$. J-K. Superposition of the new 4.2-Å resolution (GluA2 in light blue and γ5 in dark blue) and previously published 6.1-Å resolution (PDB ID: 5WEM; GluA2 in light yellow and γ5 in dark yellow) GluA2-GSG1L$_{apo}$ (J) and new 4.3-Å resolution (GluA2 in light orange and γ5 in dark orange) and previously published 8.4-Å resolution (PDB ID: 5VHZ; GluA2 in light green and γ5 in dark green) GluA2-GSG1L$_{Quis}$ (K).

Table S1. Cryo-EM data collection, refinement and validation statistics, Related to Figures 1 and 4 .

Structure	**GluA2-γ5$_{ZK}$ FL**	**GluA2-γ5$_{ZK}$ LBD-TMD**	**GluA2-γ5$_{Glu}$ FL**	**GluA2-γ5$_{Glu}$ LBD-TMD**	**GluA2-γ5$_{Quis}$ FL**	**GluA2-γ5$_{Quis}$ LBD-TMD**	**GluA2-GSG1L$_{apo}$ FL**	**GluA2-GSG1L$_{Quis}$ FL**	**GluA2-GSG1L$_{Quis}$ LBD-TMD**
EMDB accession code	EMD-24750	EMD-24751	EMD-24752	EMD-24748	EMD-24753	EMD-24754	EMD-24755	EMD-24756	EMD-24749
PDB accession code	7RZ4	7RZ5	7RZ6	7RYY	7RZ7	7RZ8	7RZ9	7RZA	7RYZ
Data collection and processing									
Magnification	81,000	81,000	81,000	81,000	81,000	81,000	105,000	105,000	105,000
Voltage (kV)	300	300	300	300	300	300	300	300	300
Electron exposure (e-/Å2)	62.5	62.5	51.18	51.18	51.1	51.1	58	58	58
Defocus range (μm)	–1 to –2	–1 to –2	–1 to –2	–1 to –2	–1 to –2	–1 to –2	–1 to –2	–1 to –2	–1 to –2
Pixel size (Å)	1.1	1.1	1.076	1.076	1.069	1.069	0.83	0.83	0.83
Symmetry imposed	C2	C2	C2	C2	C2	C2	C2	C2	C2
Micrographs	26,996	26,996	13,626	13,626	19,074	19,074	10,207	10,824	10,824
Initial particle images (no.)	7,073,223	7,073,223	3,712,556	3,712,556	5,011,050	5,011,050	1,515,005	1,627,160	1,627,160
Final particle images (no.)	134091	111,527	130,204	99056	127928	96823	124,571	118,416	113,568
Map resolution (Å)	3.6	3.3	4.4	4.4	4.2	4.1	4.15	4.26	4.15
FSC threshold	0.143	0.143	0.143	0.143	0.143	0.143	0.143	0.143	0.143
Map resolution range (Å)	3.3 to 6.9	3 to 6.4	4.1 to 8.0	4.1 to 5.7	3.9 to 8.4	3.8 to 4.8	3.8 to 11.1	4 to 13.8	3.8 to 7.2
Refinement									
Model resolution (Å)	3.6	3.3	4.4	4.4	4.2	4.1	4.15	4.26	4.15
FSC threshold	0.143	0.143	0.143	0.143	0.143	0.143	0.143	0.143	0.143
Model resolution range (Å)	3.3 to 6.9	3 to 6.4	4.1 to 8.0	4.1 to 5.7	3.9 to 8.4	3.8 to 4.8	3.8 to 11.1	4 to 13.8	3.8 to 7.2
Map sharpening B factor (Å^2)	–79.86	–39.00	–157.12	–125.84	–153.45	–128.94	–202.72	–165.46	–146.128
Model composition									
Non-hydrogen atoms	29002	16774	27922	15836	28054	16722	27938	27854	15746
Ligands	108	108	40	40	52	52	0	52	52
Sugar-NAG	56	0	0	0	0	0	0	0	0
Number of Protein residues	3,574	2,046	3,534	2,020	3,554	2,038	3,550	3,532	2,014
B factors (Å2)									
Protein	81.44	86.13	155.95	213.19	151.51	125.33	65.64	68.95	120.32
Ligands	54.27	48.57	79.51	117.92	195.83	55.34	-	64.59	115.42
r.m.s. deviations									
Bond lengths (Å)	0.0	0.01	0.00	0.00	0.01	0.00	0.01	0.01	0.00
Bond angles (°)	0.75	0.83	0.85	0.91	0.88	0.93	0.86	0.88	0.86
Validation									
MolProbity score	1.23	1.20	1.56	1.56	1.56	1.55	1.52	1.51	1.39
Clashscore	2.80	2.06	4.73	5.99	4.92	5.13	3.46	4.30	3.89
Poor rotamers (%)	0.13 %	0.12	0.27	0.35	0.53	0.46	0.26	0.40	0.12
Ramachandran plot									
Favored (%)	96.90	96.19	95.15	96.03	95.43	95.73	94.19	95.55	96.28
Allowed (%)	3.10	3.81	4.85	3.97	4.45	4.17	5.81	4.45	3.72
Outliers (%)	0	0	0	0	0.11	0.10	0	0	0